EPJ Web of Conferences **146**, 08011 (2017) DOI: 10.1051/epjconf/201714608011
ND2016

New cross sections for the ^{27}Al(p,x)^{7}Be nuclear process: Monitoring proton beam energy via the ^{22}Na/^{7}Be cross-section ratio between 45 and 200 MeV

Ferenc Szelecsényi[1,a], Gideon Francois Steyn[2], Francois Meiring Nortier[3], and Zoltán Kovács[1]

[1] Institute for Nuclear Research of the Hungarian Academy of Sciences, ATOMKI, 18/c Bem tér, 4026 Debrecen, Hungary
[2] iThemba LABS, Faure, PO Box 722, Somerset West, 7129, South Africa
[3] Los Alamos National Laboratory, PO Box 1663, Los Alamos, NM 87545, USA

Abstract. Cross sections are presented for ^{7}Be produced in the proton bombardment of natural Al up to 200 MeV and compared with previous literature data. Cross-section ratios for the ^{27}Al(p,x)^{22}Na and ^{27}Al(p,x)^{7}Be nuclear processes are also presented in the energy region 45−200 MeV, exploiting our previously reported cross sections for the ^{27}Al(p,x)^{22}Na process. The applicability for energy monitoring of proton beams by exploiting the ^{22}Na/^{7}Be cross-section ratio is discussed. Monte Carlo simulations in a simplified geometry provide additional information on activation of an Al monitor foil by secondary neutrons, indicating greater sensitivity to these neutrons by ^{24}Na as a beam monitor than ^{22}Na and ^{7}Be.

1. Introduction

Cross-section ratios of radionuclides produced in monitor foils, for well-measured nuclear reactions, provide an efficient method for energy monitoring of charged-particle beams [1–3]. Such ratios can be invaluable to determine the mean projectile energy as a function of depth inside foil stacks for excitation function measurements and/or stacked targets for radionuclide production (see e.g. [4] for an example of a multi-target stack). The present study was prompted by a need to measure energy shifts inside stacked encap-sulated targets where failure of a capsule occurred. Failure of an upstream target in a target stack can lead to significant shifts in the production energy windows of targets located downstream of the defective one, affecting not only their yields negatively but also increasing co-produced radio-contaminant levels.

In the case of an Al capsule, there already are two well-measured proton-induced reactions which cross-section ratio is suitable for monitoring purposes: ^{27}Al(p,x)^{22}Na and ^{27}Al(p,x)^{24}Na ([^{22}Na: $T_{1/2} = 2.6027$ a, $E_\gamma = 1274.54$ keV] and [^{24}Na: $T_{1/2} = 14.997$ h, $E_\gamma = 1368.63$ and 2754.01 keV]) [5]. The premise is that the magnitude of the change of an isotope ratio from the value expected (i.e. when no failure occurred) will provide useful information on a target failure, e.g. at what stage during a bombardment the failure occurred (early on, during the latter stages or somewhere in-between). The proposed method requires the radioassay of the walls of downstream target capsules, punched out and prepared as counting sources.

In the 'ratio method', cross sections of two different nuclear reactions, but originating from the same monitor foil, are normally used. However, data from the same reaction on different foils, shifted in energy but from the same bombardment, can also be useful [6]. The main advantage of cross-section ratios originating from the same measurements is that several common quantities cancel, consequently their associated uncertainties play no role, e.g. foil thickness, accumulated charge, strength of calibration sources, counting geometry, etc.

Unfortunately, the influence of the ^{27}Al(n,α)^{24}Na reaction on the ^{27}Al(p,x)^{24}Na monitor reaction is often not negligible and can be a problem at higher proton energies, when secondary neutron production becomes significant [7–9]. For these reasons, we decided to also investigate the ^{27}Na(p,x)^{7}Be process for monitoring purposes, as ^{7}Be has a convenient half-life of 53.22 d and a sufficiently strong γ-line at 477.6 keV.

Cross sections are presented here for the ^{27}Al(p,x)^{7}Be process. These values are compared with available literature data. The corresponding ^{22}Na/^{7}Be cross-section ratios are also reported. We also comment on the observed disturbance caused by secondary neutron activation to the ^{27}Al(p,x)^{24}Na process. Results of Monte Carlo simulation studies are presented to shed light on the magnitude of the interference caused by secondary neutron activation in a single Al monitor foil.

2. Experimental

The experimental details have been described in detail in Ref. [10], so only a few salient aspects will be mentioned here. The primary proton beams were un-collimated and focussed directly onto the foil stacks. Five foil stacks were activated, utilising primary proton beams with nominal energies of 200, 120, 100, 66 and 40 MeV. The stacks were bombarded inside a calibrated Faraday cup. The foil diameter was 20 mm, the stack compositions dominated by Al, which served as both degrader and monitor material. Interspersed with the Al degraders and monitor foils were

[a] e-mail: szele@atomki.hu

Ni and Mn/Ni-alloy foils, the main aim of which was to measure the ^{52}Fe excitation function in ^{nat}Ni+p and ^{nat}Mn+p. The beams were supplied by the separated-sector cyclotron of iThemba LABS, South Africa. After bombardment, the foils were counted repeatedly for their γ-ray emissions, using a calibrated intrinsic Ge detector with a relative efficiency of 13% and a resolution of 1.8 keV FWHM at 1.33 MeV.

The total uncertainties in the cross sections were obtained by summing all the contributing uncertainties in quadrature and were expressed with a 1 standard deviation (1σ) criterion. In the original paper [10], no energy uncertainties were reported along with the presented cross section data. This has now been rectified, taking into account energy straggling, target foil thicknesses as well as the estimated energy spread of the primary proton beams.

3. Results and discussion

3.1. The ^{27}Al(p,x)^{7}Be excitation function

The measured cross sections for the production of ^{7}Be in the bombardment of natural Al with protons are shown in Fig. 1, together with some selected experimental data from the literature [11–17]. Some data sets [18–21] have been omitted due to the limited space in the figure. The new values of this work are compiled in Table 1. Below 100 MeV, the majority of results from different experiments show reasonably good agreement, the values of Furukawa et al. [12] systematically lower and Miyano [14] systematically higher. Until now, only two groups reported measured cross sections up to 200 MeV (Titarenko et al. [16,17], and Michel et al. [13]). The two datasets of Titarenko not only exhibit rather large differences but also associated high uncertainties. The results of Michel show better agreement with the present work but exhibit rather large scatter above 100 MeV. It is evident that the excitation function is monotonically increasing over the studied energy region, with no discernible structures or peaks.

3.2. The ^{27}Al(p,x)^{22}Na excitation function

The ^{22}Na cross-section data of Ref. [10], extracted from the same γ-ray spectra used to produce the results of Table 1, are available in the EXFOR library (Entry A0497001). These values have been used to calculate the ^{22}Na/^{7}Be cross-section ratios presented below. This data set was used in the evaluation that led to the recommended ^{27}Al(p,x)^{22}Na monitor excitation function of the IAEA [5], with which it has excellent agreement.

3.3. The ^{27}Al(p,x)^{24} Na excitation function

As reported by several previous authors, we also found activation by secondary neutrons to be significant, in particular above 100 MeV. Differences of the order of 10% were found in the overlap region of the 200 MeV and 120 MeV stacks, the larger values obtained with the degraded 200 MeV proton beam. This is why Ref. [10] did not report a measured ^{27}Al(p,x)^{24}Na excitation function. For ^{22}Na and ^{7}Be such differences were not observed. We consequently abandoned the idea to utilise the ^{22}Na/^{24}Na ratios for energy monitoring purposes and decided on the ^{22}Na/^{7}Be ratios instead. We also agree with a statement by Kim et al. [22] who ascribed published cross-section values significantly below the threshold of the ^{27}Al(p,3pn)^{24}Na reaction to be likely due to the secondary (n,α) reaction.

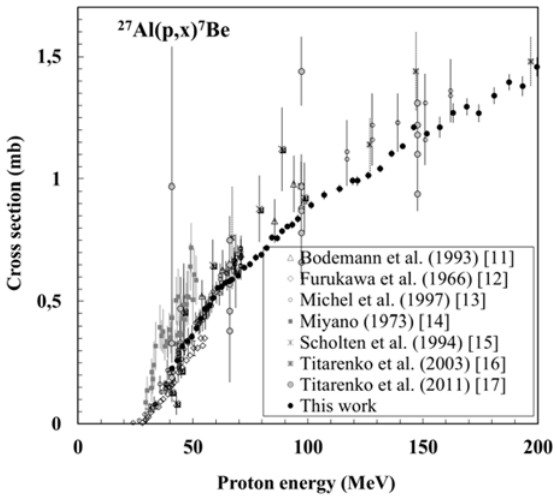

Figure 1. Cross sections for the production of ^{7}Be in ^{27}Al+p.

Table 1. Measured cross sections for the production of ^{7}Be in the proton bombardment of ^{27}Al.

Energy (MeV)	[a]Cross section (mb)	Energy (MeV)	[a]Cross section (mb)
40.94 ± 0.88	0.23 ± 0.01	88.84 ± 0.44	0.79 ± 0.02
43.22 ± 0.83	0.26 ± 0.01	91.01 ± 0.41	0.81 ± 0.01
45.41 ± 0.78	0.32 ± 0.02	93.15 ± 0.62	0.81 ± 0.01
47.52 ± 0.73	0.34 ± 0.02	95.58 ± 0.36	0.84 ± 0.01
49.56 ± 0.68	0.36 ± 0.02	101.42 ± 0.52	0.89 ± 0.04
51.54 ± 0.64	0.39 ± 0.02	107.0 3± 0.48	0.94 ± 0.04
53.47 ± 0.59	0.43 ± 0.02	113.73 ± 1.61	0.96 ± 0.04
55.35 ± 0.54	0.47 ± 0.02	119.44 ± 0.41	0.99 ± 0.04
57.18 ± 0.49	0.48 ± 0.02	121.52 ± 1.52	0.99 ± 0.04
58.97 ± 0.87	0.52 ± 0.02	126.28 ± 1.45	1.01 ± 0.03
60.72 ± 0.81	0.56 ± 0.02	131.41 ± 1.39	1.04 ± 0.04
62.43 ± 0.42	0.56 ± 0.02	136.40 ± 1.32	1.10 ± 0.04
64.10 ± 0.77	0.58 ± 0.01	141.27 ± 1.26	1.13 ± 0.04
65.74 ± 0.34	0.58 ± 0.01	146.03 ± 1.20	1.21 ± 0.05
67.04 ± 0.72	0.59 ± 0.02	151.75 ± 1.12	1.18 ± 0.04
69.71 ± 0.69	0.6 1± 0.02	157.32 ± 1.05	1.21 ± 0.03
72.31 ± 0.66	0.64 ± 0.02	163.19 ± 0.98	1.27 ± 0.03
74.83 ± 0.62	0.65 ± 0.02	169.09 ± 0.90	1.29 ± 0.03
77.30 ± 0.59	0.68 ± 0.02	174.29 ± 0.83	1.27 ± 0.03
79.70 ± 0.56	0.69 ± 0.02	180.97 ± 0.75	1.34 ± 0.04
82.06 ± 0.53	0.72 ± 0.02	187.49 ± 0.66	1.40 ± 0.04
84.36 ± 0.50	0.76 ± 0.02	193.34 ± 0.59	1.38 ± 0.03
86.62 ± 0.47	0.76 ± 0.02	199.60 ± 0.51	1.46 ± 0.03

[a]Listed uncertainties exclude a systematic uncertainty of 6%

3.4. The ^{22}Na/^{7}Be cross-section ratio

The experimental ^{22}Na/^{7}Be cross-section ratios for ^{27}Al+p are shown in Fig. 2 while the numerical values are compiled in Table 2. The ^{22}Na/^{7}Be ratios exhibit a monotonically decreasing trend with increasing energy in the 40-200 MeV energy regions. In addition, its range spans a factor of about 20, making it a sensitive monitor for proton energy in a large part of this energy region.

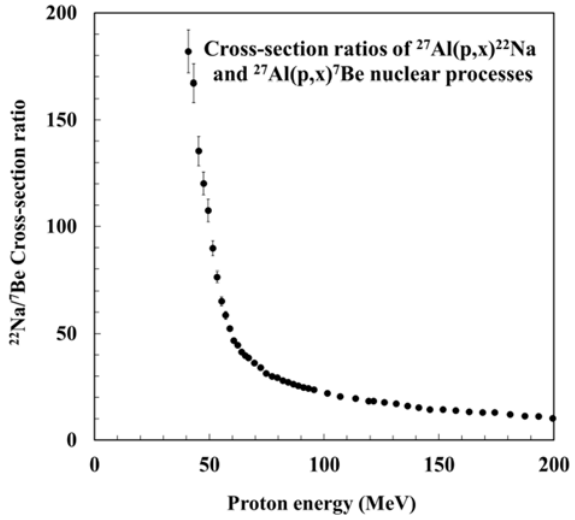

Figure 2. Experimental ^{22}Na/^{7}Be cross-section ratios for ^{27}Al+p.

Table 2. Calculated ^{22}Na/^{7}Be cross-section ratios from the ^{27}Al(p,x)^{22}Be and ^{27}Al(p,x)^{7}Be nuclear processes.

Energy (MeV)	Cross section ratio	Energy (MeV)	Cross section ratio
40.94	181.91 ± 10.1	88.84	25.41 ± 0.57
43.22	167.13 ± 9.35	91.01	24.63 ± 0.47
45.41	135.36 ± 6.83	93.15	24.31 ± 0.47
47.52	120.22 ± 5.33	95.58	23.63 ± 0.59
49.56	107.47 ± 5.23	101.42	21.99 ± 1.14
51.54	89.69 ± 3.43	107.03	20.38 ± 0.94
53.47	76.52 ± 2.64	113.73	19.54 ± 0.79
55.35	65.11 ± 2.19	119.44	18.23 ± 0.74
57.18	58.54 ± 1.86	121.52	18.29 ± 0.98
58.97	52.29 ± 1.38	126.28	17.73 ± 0.90
60.72	46.70 ± 1.30	131.41	17.00 ± 0.91
62.43	44.60 ± 1.23	136.40	16.06 ± 0.80
64.10	41.32 ± 1.08	141.27	15.16 ± 0.76
65.74	39.60 ± 0.85	146.03	14.29 ± 0.68
67.04	38.53 ± 1.24	151.75	14.38 ± 0.58
69.71	36.22 ± 1.18	157.32	13.92 ± 0.52
72.31	34.00 ± 1.00	163.19	13.31 ± 0.45
74.83	31.20 ± 0.99	169.09	12.88 ± 0.43
77.30	29.87 ± 0.84	174.29	12.88 ± 0.38
79.70	29.22 ± 0.77	180.97	11.98 ± 0.39
82.06	27.83 ± 0.79	187.49	11.28 ± 0.33
84.36	27.18 ± 0.65	193.34	11.04 ± 0.30
86.62	26.18 ± 0.61	199.60	10.26 ± 0.26

4. Monte Carlo simulations

Monte Carlo simulations were performed in an attempt to gain a better understanding of the secondary neutron activation of an Al monitor foil in a degraded proton beam. The primary beam was mono-energetic and fixed at 200 MeV, while a single Al foil of 0.1 mm thickness was located at a position where the mean beam energy was 120 MeV. Instead of modelling the entire 200 MeV foil stack used in the actual experiment [10], the upstream target material was modelled as a single, solid degrader. As the majority material in the 200 MeV foil stack of Ref. [10] was Al, a solid Al degrader was specified. A second calculation was performed using Cu as the degrader material. The Al foil (20 mm in diameter) was placed against the degrader, centered on the beam axis.

Table 3. Calculated ratios of neutron-induced to proton-induced yields of ^{24}Na, ^{22}Na and ^{7}Be formed in ^{27}Al+p.

Degrader	Nuclide	$\bar{\sigma}_n$ (mb)	σ_p (mb)	$\frac{N_n}{N_p}$	R (%)
Cu	^{24}Na	25.3	11.4	0.0820	18.2
	^{22}Na	8.72	18.1		3.95
	^{7}Be	0.0170	0.99		0.097
Al	^{24}Na	31.1	11.4	0.0301	8.21
	^{22}Na	12.8	18.1		2.13
	^{7}Be	0.0143	0.99		0.043

The forward spectra of neutrons emerging from the degraders were obtained from the MCNPX code [23] and found to be in good agreement with similar calculations performed with the FLUKA code [24,25]. Current tallies were set for both the protons and the neutrons passing through the single Al foil. From these simulations, normalized neutron spectra for the energy region 0.8 MeV to the maximum energy of emitted neutrons were obtained as well as the fluence ratio of neutrons to protons passing through the Al foil.

Excitation functions of neutron-induced reactions on ^{27}Al leading to the formation of ^{7}Be, ^{22}Na and ^{24}Na were taken from the TENDL-2015 library [26]. Effective production cross sections were calculated by folding these excitation functions with the normalized neutron spectra, given by

$$\bar{\sigma}_n = \int_{0.8}^{E_{max}} \sigma_n(E) S_n(E) dE, \quad (1)$$

where $\sigma_n(E)$ represents the TENDL-2015 data and $S_n(E)$ is a normalized neutron spectrum. This allowed the ratio of neutron-induced to proton-induced yields to be calculated as follows:

$$R = \left[\frac{\bar{\sigma}_n}{\sigma_p(120)}\right]\left[\frac{N_n}{N_p}\right] \quad (2)$$

where $\sigma_p(120)$ is the cross-section for the proton-induced reaction at an energy of 120 MeV and N_n/N_p is the ratio of neutrons to protons passing through the foil. The results are shown in Table 3.

These predictions indicate that the activity induced by secondary neutrons negatively affect ^{24}Na produced in ^{27}Al+p (as a monitor for protons) to a much larger extent than ^{22}Na and ^{7}Be, in the energy region investigated. Large uncertainties in the TENDL-2015 cross sections used cannot be ruled out, nevertheless, the results are in agreement with experimental observations.

5. Conclusion

Cross sections for the ^{27}Al(p,x)^{7}Be nuclear processes have been presented up to 200 MeV as well as experimental values for the ^{22}Na/^{7}Be ratio in ^{27}Al+p. Admittedly, the results of the Monte Carlo simulations should be interpreted with caution, even though they are in agreement with observations. Nevertheless, there is sufficient evidence that the ^{22}Na/^{7}Be ratio is better suited than the ^{22}Na/^{24}Na ratio for proton energy monitoring above about 100 MeV, as the fraction of ^{24}Na produced by secondary neutrons is substantially higher than in the cases of ^{22}Na and ^{7}Be.

This work was financially supported by the Hungarian Research Foundation (Budapest, OTKA: K108669) and the National Research Foundation (Pretoria, NRF Grant 85507).

References

[1] H. Piel, S.M. Qaim and G. Stöcklin, Radiochim Acta **57**, 1–7 (1992)
[2] J.H. Kim, H. Park, S. Kim, J.S. Lee and K. S. Chun, J. Korean Phys. Soc. **48**, 755–758 (2006)
[3] M.U. Khandaker, G. Kim, K. Kim, H.B.A. Kassim and B. Nikouravan, Int. J. Phys. Sci. **6**, 3168–3174 (2011), Available online at `http://www`. academic journals.org/IJPS
[4] N.P. van der Meulen, G.F. Steyn, C. Vermeulen and T.J. van Rooyen, Appl. Radiat. Isot. **115**, 125–132 (2016)
[5] S.M. Qaim, F.T. Tárkányi, P. Obložinský, K. Gul, A. Hermanne, M.G. Mustafa, F.M. Nortier, B. Scholten, Y. Shubin, S. Takács and Y. Zhuang, Charged-particle cross section database for medical radioisotope production (IAEA Nuclear Data Services), Available online at `https://www-nds.iaea.org/medical/`
[6] K. Gagnon, M. Jensen, H. Thisgaard, J. Publicover, S. Lapi, S.A. McQuarrie and T. Ruth, Appl. Radiat. Isot. **69**, 247–253 (2011)
[7] M. Calviani, F. Cerutti, F.P. LaTorre, G.P. Manessi, F. Pozzi, C.T. Severino and M. Silari, Prog. Nucl. Sci. Technol. **4**, 358–362 (2014)
[8] J.-S. Wan, M. Ochs, P. Vater, X.P. Song, E.-J. Langrock, R. Brandt, J. Adam, V. P. Bemblevski, B.A. Kulakov, M.I. Krivopustov, A.N. Sosnin, G. Modolo and R. Odoj, Nucl. Instr. Meth. B **155**, 110–115 (1999)
[9] R. Brandt, Ch. Gfeller and W. Stötzel-Riezier, Nucl. Instr. Meth. **62**, 109–111 (1968)
[10] G.F. Steyn, S.J. Mills, F.M. Nortier, B.R.S. Simpson and B.R. Meyer, Appl. Radiat. Isot. **41**, 315–325 (1990)
[11] R. Bodemann, H.-J. Lange, I. Leya, R. Michel, T. Schiekel, R. Rösel, U. Herpers, H.J. Hofmann, B. Dittrich, M. Suter, W. Wölfli, B. Holmqvist, H. Condé and P. Malmborg, Nucl. Instr. Meth. B **82**, 9–31 (1993)
[12] M. Furukawa, S. Kume and M. Ogawa, Nucl. Phys. **69**, 362–368 (1965)
[13] R. Michel, R. Bodemann, H. Busemann, R. Daunke, M. Gloris, H.-J. Lange, B. Klug, A. Krins, I. Leya, M. Lüpke, S. Neumann, H. Reinhardt, M. Schnatz-Büttgen, U. Herpers, Th. Schiekel, F. Sudbrock, B. Holmqvist, H. Condé, P. Malmborg, M. Suter, B. Dittrich-Hannen, P.-W. Kubik, H.-A. Synal and D. Filges, Nucl. Instr. Meth. B **129**, 153–193 (1997)
[14] K. Miyano, J. Phys. Soc. Japan **34**, 853–856 (1973)
[15] B. Scholten, S. M. Qaim and G. Stöcklin, Radiochim. Acta **65**, 81–86 (1994)
[16] Yu. E. Titarenko, O.V. Shedov, V.F. Batyaev, E.I. Karpikhin, V.M. Zhivun, A.B. Koldobsky, R.D. Mulambetov, A.N. Soshin, Yu.N. Shubin, A.V. Ignatyuk, V.P. Lunev, S.G. Mashnik, R.E. Prael, T.A. Gabriel and M. Blann, IAEA Report, INDC (CCP)-434, 86 (2003)
[17] Yu.E. Titarenko, S.P. Borovlev, M.A. Butko, V.M. Zhivun, K.V. Pavlov, V.I. Rogov, A.Yu. Titarenko, R.S. Tikhonov, S.N. Florya and A.B. Koldobskiy, Yad. Fiz. **74**, 531–547 (2011)
[18] J.M. Sisterson, K. Kim, A. Beverding, P.J.A. Englert, M.W. Caffee, J. Vincent, C. Castaneda and R.C. Reedy, AIP Conf. Proc. **392**, 811 (1997)
[19] E.F. Neuzil and R.H. Lindsay, Phys. Rev. **131**, 1697–1701 (1963)
[20] M.S. Lafleur, N.T. Porile and L. Yaffe, Can. J. Chem. **44**, 2749–2767 (1966)
[21] R. Bimbot and H. Gauvin, Compt. Rend. B **273**, 1054–1057 (1971)
[22] G.N. Kim, M.U. Khandaker, K. Kim, M.W. Lee and K.S. Kim, J. Korean Phys. Soc. **59**, 1821–1824 (2011)
[23] D.B. Pelowitz, J.W. Durkee, J.S. Elson, M.L. Fensin, J.S. Hendricks, M.R. James, G.W. McKinney, S.G. Mashnik, J.M. Verbeke, L.S. Waters and T.A. Wilcox, *MCNPX 2.7.E Extensions* (Los Alamos Report LA-UR-11-01502, 2011)
[24] T.T. Böhlen, F. Cerutti, M.P.W. Chin, A. Fasso, A. Ferrari, P.G. Ortega, A. Mairani, P.R. Sala, G. Smirnov and V. Vlachoudis, Nucl. Data Sheets **120**, 211–214 (2014)
[25] A. Ferrari, P.R. Sala, A. Fasso and J. Ranft, *FLUKA: a multi-particle transport code* (CERN-2005-10, INFN/TC_05/11, 2005)
[26] A.J Koning, D. Rochman, J. Kopecky, J. Ch. Sublet, M. Fleming, E. Bauge, S. Hilaire, P. Romain, B. Morillon, H. Duarte, S.C. van der Marck, S. Pomp, H. Sjöstrand, R. Forrest, H. Henriksson, O. Cabellos, S. Goriely, J. Leppanen, H. Leeb, A. Plompen and R. Mills, *TENDL-2015: TALYS-based Evaluated Nuclear Data Library*. Available online at `www.talys.eu`